

# Proton Kinetic Effects in Vlasov and Solar Wind Turbulence

S. Servidio<sup>1</sup>, K.T. Osman<sup>2</sup>, F. Valentini<sup>1</sup>, D. Perrone<sup>1</sup>, F.

Califano<sup>3</sup>, S. Chapman<sup>2</sup>, W. H. Matthaeus<sup>4</sup>, and P. Veltri<sup>1</sup>

<sup>1</sup>*Dipartimento di Fisica, Università della Calabria, I-87036 Cosenza, Italy*

<sup>2</sup>*Centre for Fusion, Space and Astrophysics; University of Warwick,  
Coventry, CV4 7AL, United Kingdom*

<sup>3</sup>*Dipartimento di Fisica and CNISM, Università di Pisa, 56127 Pisa, Italy*

<sup>4</sup>*Bartol Research Institute and Department of Physics and Astronomy,  
University of Delaware, Newark, DE 19716, USA*

(Dated: July 10, 2017)

## Abstract

Kinetic plasma processes have been investigated in the framework of solar wind turbulence, employing Hybrid Vlasov-Maxwell (HVM) simulations. The dependency of proton temperature anisotropy  $T_{\perp}/T_{\parallel}$  on the parallel plasma beta  $\beta_{\parallel}$ , commonly observed in spacecraft data, has been recovered using an ensemble of HVM simulations. By varying plasma parameters, such as plasma beta and fluctuation level, the simulations explore distinct regions of the parameter space given by  $T_{\perp}/T_{\parallel}$  and  $\beta_{\parallel}$ , similar to solar wind sub-datasets. Moreover, both simulation and solar wind data suggest that temperature anisotropy is not only associated with magnetic intermittent events, but also with gradient-type structures in the flow and in the density. This connection between non-Maxwellian kinetic effects and various types of intermittency may be a key point for understanding the complex nature of plasma turbulence.

PACS numbers: 52.35.Ra, 96.50.Ci, 52.65.-y, 94.05.-a, 94.05.Lk, 52.65.Ff

In magnetohydrodynamic turbulent flows, regions of strong gradients define small scale coherent structures that are expected to be sites of enhanced dissipation [1]. Such coherent structures may also be sites of magnetic reconnection and plasma heating [2]. On the other hand, in low-collisionality plasmas, such as the solar wind, it is expected that kinetic processes lead to other phenomena such as temperature anisotropy and energization of suprathermal particles [2–4]. Since solar wind plasma is generally observed to be in a strongly turbulent state it is far from clear how processes such as dissipation operate, and how observed microscopic non-equilibrium conditions are related to the dynamics and thermodynamics that influences the large scale features, including the origin and acceleration of the solar wind itself.

Far from the textbook conditions of uniform plasma equilibrium, that motivate much of the traditional discourse on plasma dissipation, the highly excited but weakly collisional solar wind demonstrates a more complex relationship between the macroscopic state and the microscopic physics than one would find in a viscous fluid. Here we explore the connections between turbulence and solar wind properties, employing Vlasov kinetic simulations. We find that the simulations are able to recover solar wind kinetic phenomena through the combined effect of reasonable variation in the initial parameters along with the natural dynamical variations produced by the turbulence itself. Therefore, we suggest that the kinetic properties of an ensemble of solar wind observations is controlled by turbulence properties.

In situ spacecraft measurements reveal that interplanetary proton velocity distribution functions (VDFs) are anisotropic with respect to the magnetic field [5]. Values of the anisotropy  $T_{\perp}/T_{\parallel}$  range broadly, with most values between  $10^{-1}$  and 10 [6, 7]. The distribution of  $T_{\perp}/T_{\parallel}$  depends systematically on the ambient proton parallel beta  $\beta_{\parallel} = n_p k_B T_{\parallel} / (B^2 / 2\mu_0)$  – the ratio of parallel kinetic pressure to magnetic pressure, manifesting a characteristic shape in the parameters plane defined by  $T_{\perp}/T_{\parallel}$  and  $\beta_{\parallel}$  [6–8]. More recently [9], observations have suggested that a link exists between anisotropy and intermittent current sheets. The latter study employed the Partial Variance of Increments (PVI) technique which provides a running measure of the magnetic field intermittency level, and is able to quantify the presence of strong discontinuities [10]. Elevated PVI values signal an increased likelihood of finding coherent magnetic structures such as current sheets, and occur in the same regions of parameter space where elevated temperatures are found [9], and also near to identified instability thresholds [7]. Hybrid-Vlasov and Particle In Cell simulations of turbulence complement these findings by establishing that kinetic effects are concentrated near regions of strong magnetic stress [11–15]. Here we further investigate this path by exploring a broad range

of plasma parameters, and establishing a more complex link between temperature anisotropy and turbulence intermittency.

Kinetic plasma turbulence is an incompletely understood problem, and treatments such as linear and quasi-linear simplifications of the Vlasov-Maxwell equations may provide useful guidance [16]. However, for plasmas found to be in a turbulent state, it is not at all obvious whether such simplified models reliably provide a valid description. On both technical and physical grounds, one might question whether linear homogeneous Vlasov theory is sufficient to explain the inhomogeneous plasma dynamics operating near coherent structures. Hence, a strong basis for analyzing the dynamics of such plasmas is provided by direct numerical simulations of plasma kinetic equations, in which the time evolution of the VDF is described self-consistently, and in the absence of particle noise (a crucial point in studying small scale gradients [17].) In turbulent systems such as the solar wind [18], it is of crucial relevance to quantify the role of kinetic effects in the turbulent cascade, since this provides a path to explain the energy dissipation mechanisms. Non-Maxwellian features of the VDF represent a direct manifestation of the underlying complex kinetic processes. Here we perform an ensemble of direct numerical simulations of the Hybrid Vlasov-Maxwell (HVM) model [19]. We compare results with solar wind datasets from the Wind spacecraft, and we investigate the structures that contribute to the local anisotropy observed in the solar wind.

We performed direct numerical simulations of a 5 dimensional (2D in space; 3D in velocity space) Vlasov model [11, 19] for protons, coupled to a fluid model for electrons. The 2D plane is perpendicular to the mean field  $B_0 \hat{z}$ , and fluctuating vectors are 3D. In order to mimic the variability of the solar wind, we vary the plasma beta, and also the level of fluctuations  $\delta b/B_0$ , where  $\delta b$  the rms fluctuation value. The simulation box is of size  $2\pi 20d_i$  ( $d_i$  is the ion skin depth), with a resolution of  $512 \times 512$  in the physical space, and a typical resolution of  $51^3$  in the velocity space. The velocity space resolution is varied for the simulations with smaller plasma beta, where we tested the results by varying the resolution from  $51^3$  to  $81^3$ . For these parameters, the conservation of the total mass and energy of the system in the simulations is satisfied with typical relative errors of  $\simeq 10^{-3}\%$  and  $\simeq 10^{-5}\%$ , respectively. As described in [11], we initialize the turbulence by specifying a band limited Gaussian spectrum of fluctuations, and an isotropic Maxwellian plasma ( $T_{\perp}/T_{\parallel} = 1$ ) with uniform temperature. The correlation length (energy containing scale) is  $\ell \simeq 10d_i$ . The range of dynamically accessible scales is a compromise due to a finite simulation size, but it includes both proton kinetic scales and extends into the fluid regime. This class of simulations evolves [11, 20] by forming a broad band spectrum extending from cor-

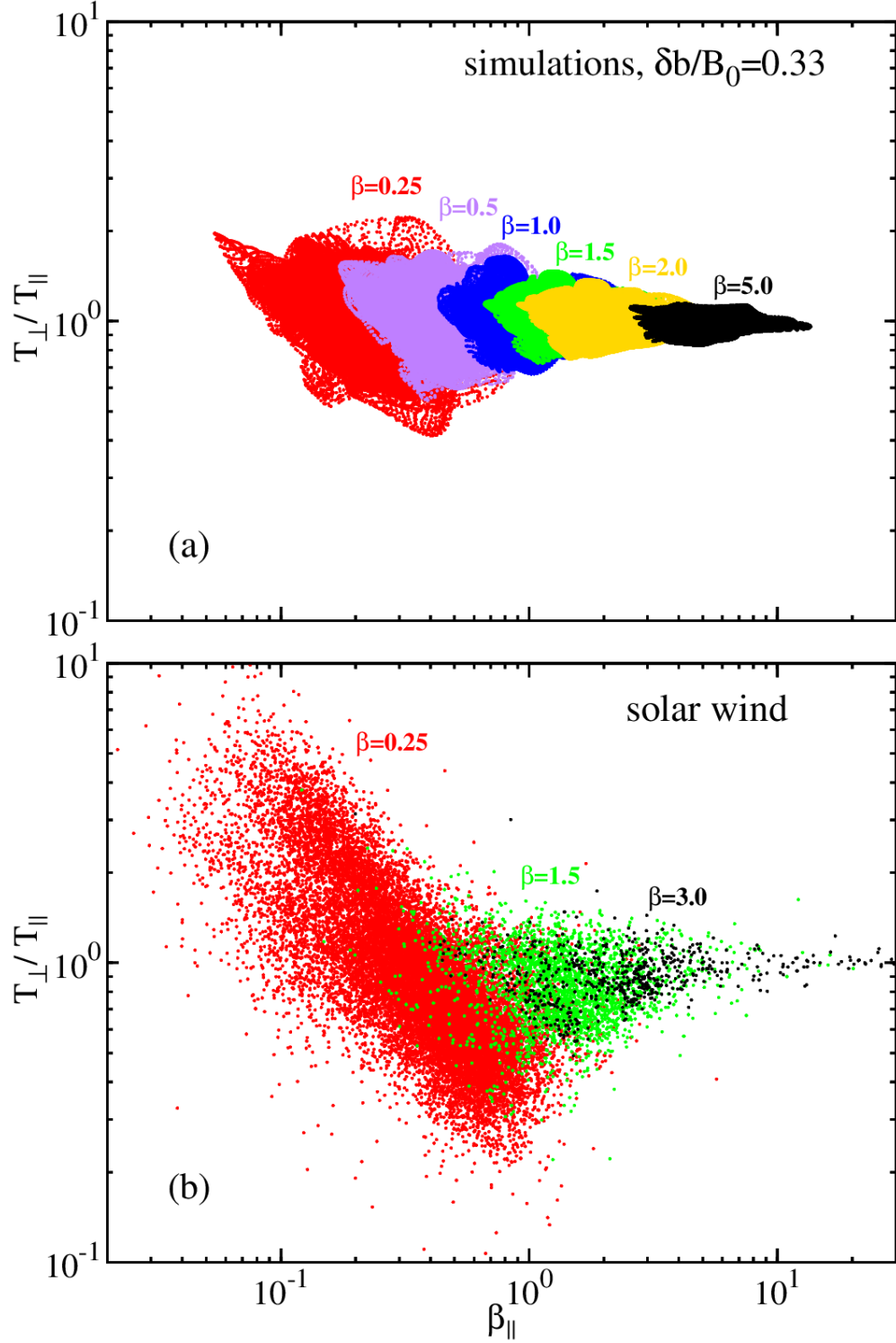


FIG. 1: (Color online) (a) Scatter plot of anisotropy  $T_{\perp}/T_{\parallel}$  vs.  $\beta_{\parallel}$  for the HVM simulations, performed with  $\delta b/B_0 = 0.33$ , and varying  $\beta = 0.25, 0.5, 1.0, 1.5, 2.0$  and  $5.0$  (from left to right). (b) Solar wind samples in the same plane, sorted in four hour samples with the average value of  $\beta = 0.25$  (red),  $1$  (green), and  $3$  (black).

relation scale  $\ell$  to kinetic scales ( $< d_i$ ), implying an effective Reynolds number, as in classical turbulence theory, on the order of  $(\ell/d_i)^{4/3}$ , while also forming characteristic small scale structures associated with intermittency. Therefore the dynamics appears to be analogous to moderately high ( $\gg 1$ ) Reynolds number strong turbulence.

For each simulation we used the data near the time of peak of nonlinear activity [11]. A scatter plot of temperature anisotropy as a function of the  $\beta_{\parallel}$  is shown in Fig. 1, for simulations initialized with  $\delta b/B_0 = 1/3$ , and with uniform initial plasma beta varying over values  $\beta = 0.25, 0.5, 1, 1.5, 2, 5$ . It is apparent that the dynamically evolved data are strongly modulated by the choice of beta, and are also spread in temperature anisotropy (note that at  $t = 0$ ,  $T_{\perp}/T_{\parallel} = 1$ ). Notably, the resulting distributions resemble the familiar form of those accumulated from years of solar wind data, as in [6, 9].

In order to further confirm our methodology, a similar analysis has been carried out using a large sample of solar wind data, binning the data according to plasma  $\beta$ . The solar wind dataset, which spans 17 years with a cadence of 92 seconds, is divided into 4-hour non-overlapping datasets (about 5 correlation lengths). These are sorted into three bins having average values of  $\beta = 0.25 \pm 0.01, 1.5 \pm 0.01, 3 \pm 0.01$ , where all the data falling outside of this range is excluded. As can be seen from Fig. 1-(b), when the data are sorted according to their average  $\beta$  in this way, the patterns of data in the plane move from left to right in the plot, spanning systematically the plane, in good agreement with the simulations. Since we know that in the simulations non-Maxwellian kinetic effects such as temperature anisotropies are concentrated in the non-Gaussian coherent structures [11], the above result confirms the major role that kinetic turbulence plays in the macroscopic distribution of non-Maxwellian effects in the solar wind.

The distribution determined from simulations shows the apparent signatures of regulation of the anisotropy frequently associated with instability thresholds, even though the envelope of the distribution appears to be somewhat further away from the reported mirror and firehose instability thresholds in the solar wind analyses [6, 7]. This suggests that the level of turbulent fluctuations, here represented by  $\delta b/B_0$ , may play another important role in the explanation of the observed anisotropy. To examine the influence of turbulence level on these distributions, we performed a set of simulations varying the level of fluctuations from  $\delta b/B_0 = 1/3$  to  $2/3$ . In Fig. 2 we compare data density (PDFs) of simulations with  $(\beta, \delta b/B_0) = (0.25, 1/3)$  and  $(0.25, 2/3)$ . It is evident that the level of fluctuations, together with the mean plasma beta, strongly influences the distribution of anisotropies in Vlasov turbulence. Similar results have been obtained for the

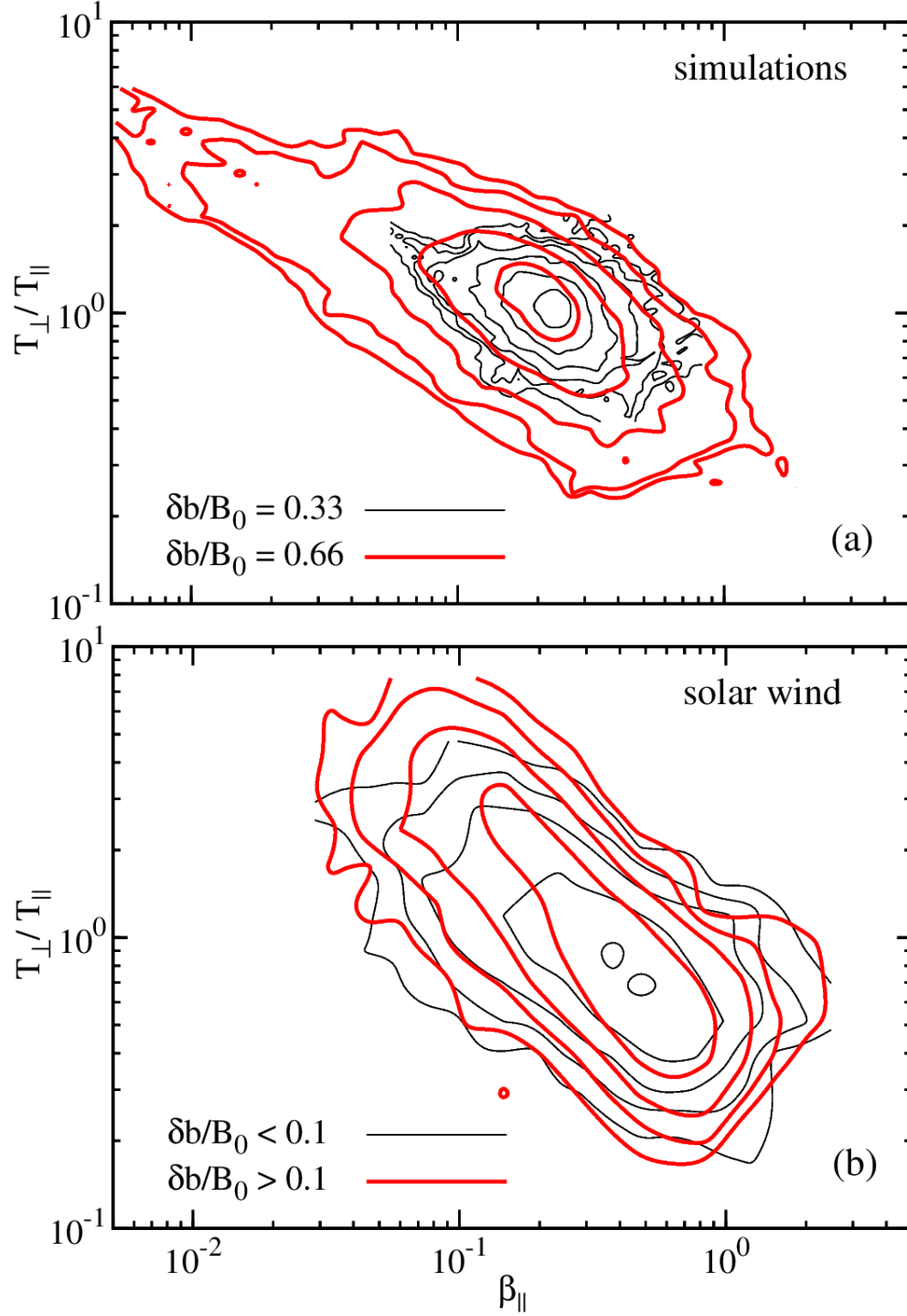


FIG. 2: (Color online) (a) Joint distributions of  $T_{\perp}/T_{\parallel}$  vs.  $\beta_{\parallel}$ , comparing simulations with  $(\beta, \delta b/B_0) = (0.25, 1/3)$  (thin-black) and  $(0.25, 2/3)$  (thick-red). (b) Samples of solar wind selected for four hour average values of  $\beta = 0.25$ , and  $\delta b/B_0 < 0.1$  (thin-black), and  $> 0.1$  (thick-red).

case with  $(\beta, \delta b/B_0) = (1, 1/3)$  and  $(1, 2/3)$  (not shown in this plot). A similar analysis has been carried out for the solar wind, sampling the data for both  $\beta$  and  $\delta b/B_0$ ; see Fig. 2 (bottom). This further confirms, especially for low beta, that the level of fluctuations plays a major role in shaping the distribution of temperature anisotropies.

A consistent interpretation of the above results is that the turbulent dynamics produces variations in kinetic anisotropies (measured here by  $T_{\perp}/T_{\parallel}$  and  $\beta_{\parallel}$ ) even when the global average values are prescribed. Furthermore, when the global average values of  $\beta$  and  $\delta b/B_0$  are varied, the dynamical spreading of local anisotropies ventures into different, and sometimes more distant regions of the parameter space. This effect is observed to be qualitatively similar in the simulations and in the solar wind analysis, keeping in mind of course that the control over parameters is direct in the former case, and obtained through conditional sampling in the latter. This interpretation may be expanded further, taking into account recent studies that show concentrations of kinetic effects near coherent structures. These effects include elevated temperatures, and enhanced kinetic anisotropies, and are seen in plasma simulations [11, 14, 15] and in solar wind observations [4, 9, 21]. One might reason in this way: intermittency is a generic feature of turbulence, leading to coherent structures of increasing sharpness at smaller scales, the effect growing stronger at higher Reynolds numbers [22]. Stronger fluctuation amplitude is associated with stronger turbulence (e.g., higher Reynolds number, larger cascade rate), and therefore for a plasma, larger  $\delta b/B_0$  should be associated with stronger intermittency and stronger small scale coherent structures. Since coherent structures are connected with kinetic anisotropies, then larger  $\delta b/B_0$  should also be connected with stronger anisotropies. A natural explanation for the current observations emerges from this line of reasoning. It is noteworthy that this is an alternative to the interpretation put forth previously [6] that the fluctuation levels are larger near the parameter space regions having larger anisotropies because instabilities that operate in those regions also act to excite these fluctuations. This interpretation provides an alternative in which the anisotropies are a consequence of the turbulence.

At this point, since from Fig. 2-(top) it is evident that each simulation has different boundaries in the anisotropy plane, it is instructive to ask whether there is an association between structures and the observed anisotropy. Such a connection was already established in the solar wind [9] based on analysis of magnetic fluctuations. Therefore recent discussion has focused on intermittency of the magnetic field and its connection to the observed anisotropy. In plasma turbulence, however, dynamical couplings may also involve structure in other fields, and other candidates for the asso-

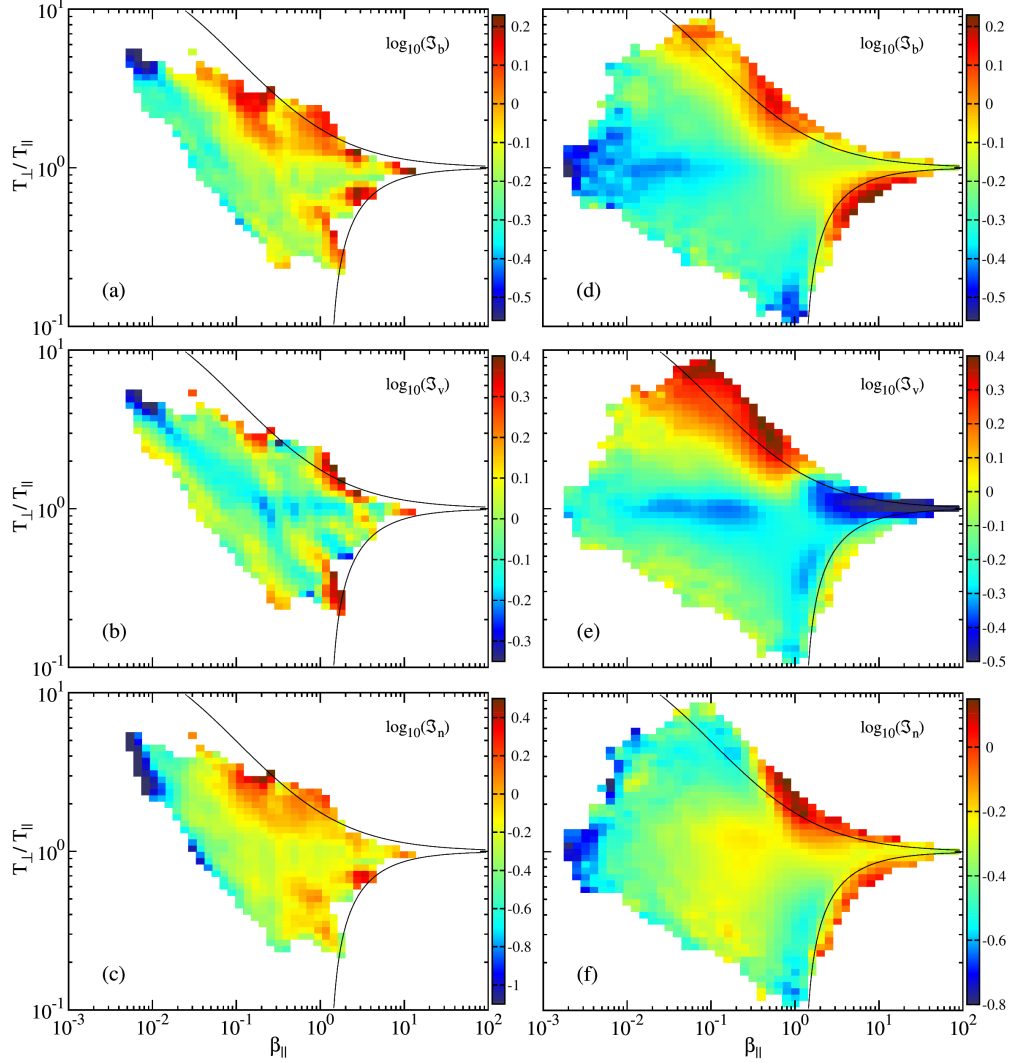


FIG. 3: (Color online) Average  $\mathfrak{S}_f$  in the anisotropy- $\beta_{\parallel}$  plane for the ensemble of simulations:  $\mathfrak{S}_b$  (a),  $\mathfrak{S}_v$  (b) and  $\mathfrak{S}_n$  (c). Same for the solar wind, in the panels (d)-(e). In each panel, dashed curves indicate theoretical growth rates for the mirror ( $T_{\perp}/T_{\parallel} > 1$ ) and the oblique firehose ( $T_{\perp}/T_{\parallel} < 1$ ) instability.

ciation with anisotropy cannot be excluded. Here we employ both simulations and solar wind data to explore this possibility, analyzing the association of magnetic, density and velocity gradients with the occurrence of strong kinetic effects.

In analogy with previous work on magnetic intermittency [10, 20], here we employ a PVI analysis for examination of flow and density gradients. This intermittency measure is given by

$$\mathfrak{S}_f(s) = \frac{|\Delta \mathbf{f}|}{\sqrt{\langle |\Delta \mathbf{f}|^2 \rangle}}, \text{ where } \Delta \mathbf{f} = \mathbf{f}(s + \Delta s) - \mathbf{f}(s), \quad (1)$$

where  $\mathbf{f}$  can be the magnetic (b) or velocity (v) vector field, or the scalar density field (n). The



brackets  $\langle \dots \rangle$  denote an appropriate time average over many correlation times (the entire simulation box, or the entire solar wind dataset). For the simulations, the variable  $s$  is a 1D variable that spans all of the simulation domain, while in the solar wind, it labels the time series at the spacecraft.

Once the data has been binned in the  $(\beta_{\parallel}, T_{\perp}/T_{\parallel})$  plane, we evaluated the average magnitude of  $\mathfrak{S}_f$  in each bin, using all the HVM simulations presented in the present work. As can be seen from Fig. 3-(a), where  $\mathfrak{S}_b$  is shown, the strongest magnetic gradients are found near the threshold regions, in agreement with [9, 11]. These can be current sheets or other discontinuities. In panel (d) of the same figure, the same analysis is shown for 17 years of solar wind data, indicating that magnetic gradients are likely playing a role in the observed anisotropy. We also performed the same analysis for the velocity field, obtaining  $\mathfrak{S}_v$ , which is a surrogate for the vorticity of the flow. It can be seen in Fig. 3-(b) that intermittency of the velocity is also strongly correlated to kinetic anisotropy. The signatures are once again near the boundaries of the characteristic anisotropy plot. Finally, the bottom panels of Fig. 3 report the same analyses for  $\mathfrak{S}_n$ , and the results qualitatively resemble the magnetic and velocity field cases. It is noteworthy that the PVI analyses of velocity and density for the solar wind cases, Fig. 3 (d)-(e), also show interesting features near the boundaries. Note that apart from the reasonable agreement in the shape of the distributions, the values of the  $\mathfrak{S}$  field are comparable between the simulations and solar wind data. Note also that the simulations show a more discontinuous behavior of the PVI very probably due to the discretization of the simulation. This effect will eventually disappear for a much higher number of simulations, that would finally realize the ergodicity of the solar wind.

These analyses converge essentially toward the same conclusions, namely that in plasma turbulence there is a strong link between intermittent structures and kinetic anisotropy. The multiple analyses presented here suggests that the intermittent structures, both magnetic and kinetic, may be central ingredients in sustaining the observed anisotropy. For example, structures may locally be found in near-equilibrium conditions, and in the absence of collisions, such configurations might require a certain amount of temperature anisotropy [23].

The present study demonstrates further that it is possible to extract statistical features from kinetic plasma simulations that motivate interpretations of solar wind behavior based on fully nonlinear plasma physics. Such studies may be carried out without recourse to extreme assumptions such as uniform plasma equilibria or linear Vlasov waves and instabilities. Here we employed nonlinear Hybrid-Vlasov simulations in 2.5 dimensions to show that: (1) the initially controlled

average plasma beta and fluctuation level produces turbulent dynamics that leads to a pointwise spread in the  $(\beta_{\parallel}, T_{\perp}/T_{\parallel})$  plane, reminiscent of solar wind populations in the same parameter plane; (2) simulations with moderate variations of average  $\beta$  and  $\delta b/B_0$  lead to fuller coverage of the  $(\beta_{\parallel}, T_{\perp}/T_{\parallel})$  plane, a tendency that is reproduced by conditional sampling of a large number of solar wind datasets; (3) that the simulations naturally lead to stronger  $\delta b/B_0$  near the boundaries of the distribution; and (4) that the extreme regions of the distribution of points in  $(\beta_{\parallel}, T_{\perp}/T_{\parallel})$  plane also show enhanced values of magnetic field gradients, velocity shears, and density gradients. All of these features, corroborated here by observations, point to an interpretation in which the appearance of large kinetic anisotropies is connected to intermittent turbulence, and the dynamical appearance of coherent structures where intense anisotropy is produced.

In the present analysis we have not been able to examine additional effects that may also be important in controlling kinetic anisotropies. For example, three dimensional effects may contribute in significant ways. The kinetic response of electrons, not explored here, may be interesting as well and has been recently implicated in producing coherent structures (see e.g., [15]). Finally, it is known that expansion produces important and systematic effects in the solar wind that have a major impact on the evolution of kinetic anisotropy; see e.g., [24]. Further and more elaborate simulations and analysis will be required to incorporate all of these effects in a single study. However, we suspect that greater realism will show additional effects while the basic features we have described will persist: intermittent turbulence and coherent structures have significant influence on the development of kinetic effects in a low collisionality plasma such as the solar wind.

This research was partially supported by the Turboplasmas project (Marie Curie FP7 PIRSES-2010-269297), POR Calabria FSE 2007/2013, the NASA Magnetosphere Multiscale Mission Theory and Modeling program NNX08AT76G, UK STFC, the Solar Probe Plus ISIS project, the NSF SHINE (AGS-1156094) and Solar Terrestrial (AGS-1063439) Programs, MIUR (PRIN 2009, 20092YP7EY). Numerical simulations were performed on the FERMI supercomputer at CINECA (Bologna, Italy) within the European project PRACE Pra04-771.

---

[1] P. Veltri, *Plasma Phys. Control. Fusion* **41** A787 (1999).

[2] E. Marsch, *Living Rev. Solar Phys.* **3**, 1 (2006); E. N. Parker, *Astrophys. J.* **330**, 474 (1988).

[3] S. P. Gary, *Theory of Space Plasma Microinstabilities* (Cambridge University Press, Cambridge,

- 1993); P. Hellinger *et al.*, *Geophys. Res. Lett.* **33**, L09101 (2006).
- [4] K. T. Osman *et al.*, *Astrophys. J. Lett.* **727**, L11 (2011).
- [5] E. Marsch *et al.*, *J. Geophys. Res.* **87**, 52 (1982); C.-Y. Tu, E. Marsch, and Z.-R. Qin, *J. Geophys. Res.* **109**, A05101 (2004).
- [6] S. D. Bale *et al.*, *Phys. Rev. Lett.* **103**, 211101 (2009).
- [7] B. A. Maruca, J. C. Kasper, and S. D. Bale, *Phys. Rev. Lett.* **107**, 201101 (2011).
- [8] J. C. Kasper, A. J. Lazarus, and S. P. Gary, *Geophys. Res. Lett.* **29**, 20 (2002).
- [9] K. T. Osman *et al.*, *Phys. Rev. Lett.* **108**, 261103 (2012).
- [10] A. Greco *et al.*, *Geophys. Res. Lett.* **35**, L19111 (2008).
- [11] S. Servidio *et al.*, *Phys. Rev. Lett.* **108**, 045001 (2012).
- [12] J. F. Drake *et al.*, *Astrophys. J.* **709**, 963 (2010).
- [13] D. Perrone *et al.*, *Astrophys. J.* **762**, 99 (2013).
- [14] M. Wan *et al.*, *Phys. Rev. Lett.* **109**, 195001 (2012); P. Wu *et al.*, *Astrophys. J. Lett.* **763**, L30 (2013).
- [15] H. Karimabadi *et al.*, *Phys Plasmas* **20**, 012303 (2013).
- [16] R. C. Davidson, *Physics of Nonneutral Plasmas* (Addison-Wesley, Redwood City, CA, 1990).
- [17] C. T. Haynes, D. Burgess, and E. Camporeale, arXiv:1304.1444 (2013).
- [18] R. Bruno and V. Carbone, *Living Rev. Solar Phys.* **2**, 4 (2005); F. Sahraoui *et al.*, *Phys. Rev. Lett.* **102**, 231102 (2009).
- [19] F. Valentini *et al.*, *J. Comput. Phys.* **225**, 753 (2007).
- [20] A. Greco *et al.*, *Phys. Rev. E* **86**, 066405 (2012).
- [21] K. T. Osman *et al.*, *Phys. Rev. Lett.* **108**, 261102 (2012).
- [22] K. R. Sreenivasan and R. A. Antonia, *Ann. Rev. Fluid Mech.* **29**, 435 (1997).
- [23] A. B. Mikhailovskii, *Theory of plasma instabilities, Vol. 2: Instabilities in an inhomogeneous plasma* (Plenum, New York, 1974).
- [24] P. Hellinger and P. M. Trávníček, *J. Geophys. Res.* **113**, A10109 (2008); L. Matteini *et al.*, *Space Sci. Rev.* **172**, 373 (2012).